Acta Pharmaceutica Sinica B 2022;12(5):2391–2405

Chinese Pharmaceutical Association
Institute of Materia Medica, Chinese Academy of Medical Sciences

Acta Pharmaceutica Sinica B

www.elsevier.com/locate/apsb
www.sciencedirect.com

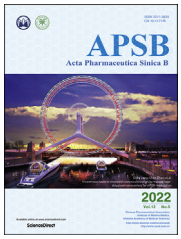

ORIGINAL ARTICLE

PXR activation impairs hepatic glucose metabolism partly *via* inhibiting the HNF4α–GLUT2 pathway

Peihua Liu[a], Ling Jiang[a], Weimin Kong[a], Qiushi Xie[a], Ping Li[a], Xiaonan Liu[a], Jiayi Zhang[a], Ming Liu[a], Zhongjian Wang[b], Liang Zhu[a], Hanyu Yang[a], Ying Zhou[a], Jianjun Zou[c,*], Xiaodong Liu[a,*], Li Liu[a,*]

[a]*Center of Drug Metabolism and Pharmacokinetics, School of Pharmacy, China Pharmaceutical University, Nanjing 210009, China*
[b]*Jiangsu Key Laboratory of New Drug Research and Clinical Pharmacy, Xuzhou Medical University, Xuzhou 221004, China*
[c]*Department of Clinical Pharmacology, Nanjing First Hospital, Nanjing Medical University, Nanjing 210006, China*

Received 14 July 2021; received in revised form 5 September 2021; accepted 16 September 2021

KEY WORDS

Pregnane X receptor;
Hepatocyte nuclear factor 4-alpha;
Glucose transporter 2;
Hepatic glucose uptake;
Diabetes;
Drug-induced hyperglycemia

Abstract Drug-induced hyperglycemia/diabetes is a global issue. Some drugs induce hyperglycemia by activating the pregnane X receptor (PXR), but the mechanism is unclear. Here, we report that PXR activation induces hyperglycemia by impairing hepatic glucose metabolism due to inhibition of the hepatocyte nuclear factor 4-alpha (HNF4α)–glucose transporter 2 (GLUT2) pathway. The PXR agonists atorvastatin and rifampicin significantly downregulated GLUT2 and HNF4α expression, and impaired glucose uptake and utilization in HepG2 cells. Overexpression of PXR downregulated GLUT2 and HNF4α expression, while silencing *PXR* upregulated HNF4α and GLUT2 expression. Silencing *HNF4α* decreased GLUT2 expression, while overexpressing HNF4α increased GLUT2 expression and glucose uptake. Silencing *PXR* or overexpressing HNF4α reversed the atorvastatin-induced decrease in GLUT2 expression and glucose uptake. In human primary hepatocytes, atorvastatin downregulated *GLUT2* and *HNF4α* mRNA expression, which could be attenuated by silencing *PXR*. Silencing *HNF4α* downregulated *GLUT2* mRNA expression. These findings were reproduced with mouse primary hepatocytes. *Hnf4α* plasmid increased *Slc2a2* promoter activity. *Hnf4α* silencing

*Corresponding authors. Tel./fax: +86 25 8327 1060.
E-mail addresses: liulee@cpu.edu.cn (Li Liu), xdliu@cpu.edu.cn (Xiaodong Liu), zoujianjun100@126.com (Jianjun Zou).
Peer review under responsibility of Chinese Pharmaceutical Association and Institute of Materia Medica, Chinese Academy of Medical Sciences.

https://doi.org/10.1016/j.apsb.2021.09.031

or pregnenolone-16α-carbonitrile (PCN) suppressed the *Slc2a2* promoter activity by decreasing HNF4α recruitment to the *Slc2a2* promoter. Liver-specific *Hnf4α* deletion and PCN impaired glucose tolerance and hepatic glucose uptake, and decreased the expression of hepatic HNF4α and GLUT2. In conclusion, PXR activation impaired hepatic glucose metabolism partly by inhibiting the HNF4α–GLUT2 pathway. These results highlight the molecular mechanisms by which PXR activators induce hyperglycemia/diabetes.

1. Introduction

Drug-induced hyperglycemia/diabetes has become a global issue, contributing to the rising prevalence of diabetes worldwide[1]. Therapeutically prescribed drugs including glucocorticoids, cholesterol-lowering statins, antipsychotics, antidepressants, antiepileptics, antiretrovirals, antibacterials, antimycobacterials, immunosuppressants, and antineoplastics have clinical diabetogenic potential with different mechanisms[2,3]. Importantly, drugs such as dexamethasone[4], atorvastatin, simvastatin, ritonavir[5], quetiapine[6], rifampicin, and phenytoin, are also activators of the pregnane X receptor (PXR). In the clinic, PXR activating drugs such as rifampicin[7], phenytoin[8], ritonavir[9], quetiapine[10], atorvastatin[11,12], and St. John's wort[13] have been reported to impair glucose tolerance. For example, 1-week treatment with rifampicin[7] or 21-day treatment with St. John's wort[13] impaired glucose tolerance in healthy volunteers. Similarly, in patients with type 2 diabetes complicated by hyperlipidemia, 3-month treatment with atorvastatin also significantly increased arbitrary blood glucose levels from 147 ± 51 (before treatment) to 176 ± 69 mg/dL[11]. Animal experiments have also shown that the PXR agonists pregnenolone-16α-carbonitrile (PCN) and atorvastatin increased glucose levels in an oral glucose tolerance test (OGTT)[7,14,15]. Although the roles of PXR in drug-induced hyperglycemia/diabetes have been demonstrated[7–10,13,14,16–18], the real mechanisms by which PXR activators impair glucose metabolism are not fully understood. PCN and atorvastatin were reported to impair glucose tolerance by impairing hepatic glucose metabolism, which was partly attributed to downregulated expression of the hepatic glucose transporter 2 (GLUT2/SLC2A2) and glucokinase (GCK)[14,15]. In HepG2 cells, rifampicin and atorvastatin were reported to impair glucose metabolism and glucose uptake by downregulating protein expression of GLUT2 and GCK, which were attenuated by PXR inhibitors or silencing *PXR*. Similarly, PXR inhibitors also reversed downregulated expression of GLUT2 and GCK and the impairment of glucose utilization in PXR-overexpressing HepG2 cells. These results demonstrate that PXR activators induce hyperglycemia partly by impairing hepatic glucose metabolism. However, the molecular mechanisms by which PXR activators impair GLUT2- and GCK-mediated glucose metabolism are not fully elucidated.

The liver plays an important role in systemic glucose homeostasis by controlling glucose uptake, glucose utilization, gluconeogenesis, glycogenesis, and glycogenolysis. In the postprandial state, glucose is taken into hepatocytes by GLUT2 and phosphorylated by GCK, then oxidized or incorporated into glycogen. GLUT2 is the predominant glucose transporter in hepatocytes in humans and rodents[19,20]. The contribution of hepatic glucose uptake to postprandial glycemic control has been demonstrated[21,22], which accounts for 60%−65% of an oral glucose load, indicating that impairment of GLUT2-mediated hepatic glucose uptake may elevate postprandial glycemia. Several studies have supported these conclusions. *Glut2* deletion was reported to impair uptake of 2-deoxy-2-[fluorine-18]-fluoro-D-glucose (^{18}F-FDG) in the livers of mice[23]. In line with this finding, portal vein glucose infusion induced a paradoxical hypoglycemic state in wild-type mice, but generated transient hyperglycemia in *Glut2*$^{-/-}$ mice[24]. Similarly, *Glut2*$^{-/-}$ mice showed elevated basal glucose levels with a sharp increase in glucose following an oral glucose dose and persistent hyperglycemia compared with wild-type mice[25,26]. The *Glut2*$^{-/-}$ mice also developed glucose intolerance following an intraperitoneal glucose dose[27] without affecting glucose production[25,27].

In general, PXR regulates the expression of its target genes by cross-talk with other nuclear receptors[16,28,29]. For instance, PXR suppresses expression of cholesterol 7-α hydroxylase and sterol 12-α hydroxylase by cross-talk with hepatocyte nuclear factor 4-alpha (HNF4α)[30]. Hepatic HNF4α, as a master regulator of liver-specific gene expression, is essential for adult and fetal liver function[31]. Our pre-experiments showed that both rifampicin and atorvastatin suppressed the protein expression of HNF4α, which was linked to downregulated protein expression of GLUT2 in HepG2 cells. Silencing *PXR* upregulated the expression of HNF4α and GLUT2, while overexpression of PXR downregulated expression of HNF4α and GLUT2. Moreover, silencing *HNF4α* also downregulated expression of GLUT2 in HepG2 cells. These results indicate that PXR activation impairs hepatic glucose uptake possibly by inhibiting the HNF4α–GLUT2 pathway.

The aim of this study was 1) to investigate systematically whether PXR activation impairs hepatic glucose metabolism by inhibiting the HNF4α–GLUT2 pathway; 2) to investigate how HNF4α regulates hepatic GLUT2 expression and hepatic glucose uptake using HepG2 cells, human primary hepatocytes and mouse primary hepatocytes; 3) to further confirm the role of the PXR–HNF4α–GLUT2 pathway in the impairment of hepatic glucose metabolism by PXR activation using mice treated with PCN and mice with a liver-specific knockdown of *Hnf4α*. The results illustrate the importance of the PXR–HNF4α–GLUT2 pathway in the impairment of hepatic glucose metabolism and the molecular mechanisms by which PXR activators induce hyperglycemia/diabetes.

2. Materials and methods

2.1. Reagents

Atorvastatin calcium and sodium pyruvate solution were purchased from Sigma−Aldrich (Shanghai, China). Rifampicin, metformin hydrochloride, phloretin, dexamethasone, and heparin sodium salt were purchased from Aladdin Industrial Corporation (Shanghai, China). PCN was purchased from Santa Cruz Biotechnology (Santa Cruz, CA, USA). ^{18}F-FDG injection was obtained from Dongcheng AMS Pharmaceutical Co., Ltd. (Nanjing, China). Dulbecco's modified Eagle medium (DMEM, high glucose; DMEM, no glucose, no glutamine, and no phenol red), Williams' medium E, Opti-MEM, non-essential amino acids (NEAA 100×), fetal bovine serum (FBS), 0.25% trypsin-EDTA, and insulin-transferrin-selenium (ITS) were purchased from GBICO (Grand Island, NY, USA). 2-(*N*-(7-Nitrobenz-2-oxa-1,3-diazol-4-yl)amino)-2-deoxyglucose (2-NBDG) and Lipofectamine 3000 transfection reagent were obtained from Invitrogen (Carlsbad, CA, USA). RNAiso Plus Reagent was purchased from Takara Biomedical Technology (Beijing, China). XenoLight RediJect 2-DG-750 probe was purchased from PerkinElmer (Waltham, MA, USA). Kits for glucose, triglyceride (TG), aspartate aminotransferase (AST), alanine aminotransferase (ALT), and alkaline phosphatase (AKP) determination were purchased from Nanjing Jiancheng Bioengineering Institute (Nanjing, China). Radioimmunoprecipitation (RIPA) lysis buffer, immunoprecipitation (IP) lysis buffer, and bicinchoninic acid (BCA) protein assay kit were purchased from Beyotime Institute of Biotechnology (Nanjing, China). Protein A/G mix magnetic beads, Rat/Mouse Insulin ELISA kit, and EZ-Magna ChIP kit were obtained from Millipore (Burlington, MA, USA). Dual-luciferase reporter gene assay kit was obtained from Promega Corporation (Madison, WI, USA).

2.2. Animals

Six to eight-week-old male C57BL/6J mice were purchased from CAVENS Lab Animal Ltd. (Changzhou, China). The mice were housed in plastic cages with free access to tap water and regular chow in a temperature-controlled facility with a 12-h light/dark cycle. All procedures on animals were carried out in accordance with guidelines on the Care and Use of animals developed by the National Advisory Committee for Laboratory Animal Research. All animals received humane care and their use was approved by the Animal Ethics Committee of China Pharmaceutical University (Nanjing, China).

2.3. Cell culture and drug treatment

HepG2 cells were from the Chinese Academy of Medical Sciences (Shanghai, China), HepG2-NR1I2, a stable cell line expressing human PXR, was established by Viewsolid Biotechnology (Beijing, China). Both HepG2 and HepG2-NR1I2 cells were cultured in DMEM supplemented with 10% FBS, 1% NEAA, antibiotics (100 IU/mL penicillin and 100 μg/mL streptomycin), and 3.7 g/L of $NaHCO_3$ in an atmosphere of 5% CO_2 at 37 °C. At 70% confluence, the cells were incubated with medium containing the tested agents for the designated times to assess glucose uptake, glucose consumption, and expression of the target proteins and genes.

Cryopreserved human hepatocytes (Cat. No. BQH1000.H15+) from nine donors were purchased from Shanghai Quan Yang Co., Ltd. (Shanghai, China) and seeded according to the instruction manual. Following overnight attachment, the medium was replaced with OptiCulture Hepatocyte Media (XenoTech, Kansas City, USA) containing atorvastatin or vehicle for another 24 h. The cultured cells were used to measure expression of the target genes.

Mouse primary hepatocytes were isolated from 6–8-week-old male C57BL/6J mice using an *in situ* liver perfusion according to a method previously described[32]. The isolated primary hepatocytes were cultured in Williams' medium E supplemented with ITS, dexamethasone (10 ng/mL), and antibiotics for 12 h. Then the cells were incubated with medium containing the tested agents for assessing glucose uptake/production and expression of the target proteins and genes.

2.4. Glucose consumption

HepG2 cells were seeded into 24-well plates at a density of 1×10^5 cells/well. At 70% confluence, the cells were incubated with atorvastatin (1, 5, and 10 μmol/L), metformin (2 mmol/L) for 24 h, or rifampicin (10 and 25 μmol/L) for 72 h, respectively. The incubation time and concentrations of the tested agents were designed based on preliminary experiment and a previous report[14], respectively. Metformin was used as a positive control. The treated cells were then exposed to fresh medium containing the same concentrations of tested agents and insulin (10 nmol/L) for another 6 h. The glucose concentration in the culture medium was determined using a glucose assay kit. Glucose consumption was calculated by subtracting the glucose content in cell-containing wells from the glucose concentrations of blank wells. Cellular protein concentrations were determined using BCA protein assay kit.

2.5. Glucose uptake

Cellular glucose uptake was evaluated using 2-NBDG as an indicator. Briefly, HepG2 cells and mouse primary hepatocytes were seeded in 24-well plates at a density of 1×10^5 cells/well. HepG2 cells were maintained in DMEM with 10% FBS to reach 70% confluence and then exposed to phloretin (20 μmol/L), atorvastatin (1, 5, and 10 μmol/L) for 24 h and rifampicin (10 and 25 μmol/L) for 72 h. Primary hepatocytes were treated with phloretin (20 μmol/L) and PCN (5, 10, and 20 μmol/L) for 48 h. Subsequently, the culture medium was replaced with glucose- and phenol red-free DMEM containing 2-NBDG (20 μmol/L for HepG2 cells, 50 μmol/L for primary hepatocytes) and tested agents following washing twice with pre-warmed phosphate buffered saline (PBS). The plate was incubated for 30 min at 37 °C and uptake was terminated by washing twice with ice-cold PBS. Uptake of 2-NBDG by cells was indexed as fluorescence intensity on a BioTek microplate reader (excitation/emission = 485/544 nm) and normalized to total cellular protein content.

2.6. Glucose production in primary hepatocytes

Primary mouse hepatocytes were seeded in 24-well plates at a concentration of 1×10^5 cells/well and were then exposed to PCN (10 μmol/L), dexamethasone (0.5 μmol/L), and metformin (2 mmol/L) for 24 h. After incubation, cells were washed with PBS and starved in glucose- and phenol red-free DMEM for 30 min to deplete cellular glycogen. Subsequently, medium was replaced with glucose- and phenol red-free DMEM containing gluconeogenic substrates (20 mmol/L sodium lactate, 2 mmol/L sodium pyruvate, and 15 mmol/L HEPES) and tested agents for another 2 h incubation. Cell supernatant was collected and glucose concentration was determined using an HPLC method described previously[33].

2.7. In vitro transfection

The human and mouse *PXR* siRNAs were purchased from Santa Cruz Biotechnology. Peroxisome proliferator-activated receptor gamma coactivator 1 alpha (*Pgc1α*) siRNA (On-target plus mouse *Pgc1α* siRNA) was purchased from Dharmacon (Lafayette, CO, USA). Human and mouse *HNF4α* siRNA and scrambled siRNA (Supporting Information Table S3) were designed and synthesized by GenePharma (Shanghai, China). For *PXR*, *HNF4α*, and *PGC1α* knockdown, HepG2 cells or primary hepatocytes were transfected with 90 nmol/L siRNA using Lipofectamine 3000 transfection reagent according to the instructions. Transfected cells were used for assay 48 h post-transfection and silencing efficiency was verified by Western blot. Scrambled siRNA was used as a negative control.

For HNF4α overexpression, human *HNF4α* and mouse *Hnf4α* cDNA sequences were cloned into the plvx plasmid (constructed by Sangon Biotechnology, Shanghai, China) and pEX-3 plasmid (constructed by Genomeditech Co., Ltd., Shanghai, China), respectively. HepG2 cells or primary hepatocytes were seeded and maintained in the appropriate medium for 12 h. Then, cells were transfected with the *HNF4α*/*Hnf4α* overexpression plasmid using Lipofectamine 3000 transfection reagent according to the product instructions. Empty vectors (plvx or pEX-3) were transfected as a control. Cells were incubated for an additional 48 h before tested agent treatment.

2.8. Effects of PCN on glucose metabolism and expression of enzymes/transporters related to glucose metabolism and glucose uptake in the livers of mice

Eight-week-old male C57BL/6J mice were randomly divided into a control group and a PCN-treated group. After 1 week of acclimation, the PCN-treated mice were intraperitoneally (i.p.) injected with 50 mg/kg PCN (dissolved in corn oil plus 30% DMSO) once a day for 5 days. The control mice received only vehicle (corn oil plus 30% DMSO).

An intraperitoneal glucose tolerance test (IPGTT) was performed on the 5th day following PCN treatment. All mice were fasted for 12 h prior to the test and fasting glucose levels were measured before glucose loading. Each mouse was administered glucose (2 g/kg) by i.p. injection and blood glucose levels were measured on an Accuchek performa glucometer (Roche Diagnostics, Basel, Switzerland) at 0, 15, 30, 60, and 90 min post glucose dose by tail tip cut.

Twenty-four hours after the last dose of PCN, mice were fasted for 6 h and then killed. Blood samples were collected for assessment of fasting plasma insulin (FINS) and glucose (FPG). The plasma insulin concentration was determined using a rat/mouse insulin ELISA kit. Homeostasis model assessment of insulin resistance (HOMA-IR) was calculated by formula HOMA-IR = FPG (mmol/L) × FINS (mU/L)/22.5. Liver samples were quickly obtained and weighed for measuring expression of target proteins and genes.

Another group of PCN-treated mice were used for assessing hepatic glucose uptake using the RediJect 2-DG-750 probe, a nonradioactive fluorescent-tagged glucose molecule developed by PerkinElmer, according to previous reports[34,35]. Briefly, on the 5th day and with an overnight fast, the mice received intravenously 100 μL probe (RediJect 2-DG-750) through the femoral vein under isoflurane anesthesia. The mice were killed at 10 min after dosing. The dose of RediJect 2-DG-750 and time were determined by a preliminary experiment. The liver and heart were quickly obtained. Fluorescence of RediJect 2-DG-750 was measured using an IVIS spectrum *in vivo* imaging system (PerkinElmer, MA, USA) with excitation and emission wavelengths of Ex (745 nm)/Em (800 nm) and images were analyzed by Living Image software. Fluorescence intensity was normalized to photons per second per centimeter square per steradian and expressed as total radiant efficiency [p/s/cm^2/sr]/[μW/cm^2][36].

2.9. Effect of liver-specific Hnf4α knockdown on glucose metabolism and expression of enzymes/transporters related to glucose metabolism and glucose uptake in the livers of mice

Six-week-old male C57BL/6J mice received adeno-associated virus serotype 8 (AAV8)-*Hnf4α*-shRNA (constructed by Genomeditech) by intraportal vein injection. For construction of AAV8-*Hnf4α*-shRNA, three shRNA sequences (Table S3) were designed for *Hnf4α* and their knockdown efficiency was determined *in vitro* using mouse primary hepatocytes. Sequence #2 was chosen as it had the greatest knockdown efficiency. A short hairpin RNA encoding sequence #2 was cloned into the BamHI and EcoRI sites of GPAAV-HU6-MCS-CMV-eGFP-WPRE vector. AAV vectors were packaged into AAV8 capsids using pHelper and pAAV-RC8 by triple transfection of AAV-293 cells, and then purified by iodixanol gradient centrifugation. Titers of the rAAV8 vectors were measured by quantitative real-time PCR (qRT-PCR). For AAV8 intraportal vein injection, mice were anesthetized with isoflurane after overnight fasting. The portal vein was exposed by midline abdominal incision and a 200 μL volume of virus/PBS mixture (5×10^{11} vector genomes) was slowly injected into the portal vein over a period of 1 min using an insulin syringe. After injection, a small piece of absorbable sponge was gently pressed over the insertion point to staunch bleeding. Then abdominal incision was closed. Following the surgery, the mice continued to feed for 23 days.

On the 22nd day, an IPGTT was performed as described above. On the 23rd day, the mice were killed and blood samples were collected for measuring FINS and FPG following a 6-h fast. Liver samples were collected and weighed for measuring the expression of target proteins and genes.

Another group of liver-specific *Hnf4α* knockdown mice were generated to evaluate glucose-stimulated insulin secretion (GSIS) after oral glucose challenge. The mice were fasted for 12 h and

received an oral dose of glucose (2 g/kg). Blood samples were collected at 0 (before dose) and 15, 30, 60, and 90 min post-glucose loading for measuring insulin and glucose levels in the plasma.

Micro-positron emission tomography/computed tomography (PET/CT) was used to measure hepatic ^{18}F-FDG uptake in liver-specific *Hnf4α* knockdown mice. Briefly, on the 22nd day following AAV8-*Hnf4α*-shRNA injection, mice were fasted overnight and anesthetized with 1.5% isoflurane. Mice were then positioned on a heated custom PET/CT small animal holder, which allowed for continuous anesthesia. ^{18}F-FDG (37 MBq) was injected as a bolus through the femoral vein and 15-min dynamic PET scans were performed at 2 min after injection on an Inveon Micro-PET/CT (Siemens Medical Solutions, Erlangen, Germany). For dynamic scans, the acquired data were sorted into 5-s frames for 2 min; 30-s frames for 3 min; 2-min frames for 10 min. PET acquisition was immediately followed by a CT scan to provide anatomical information. Images were reconstructed by a 3-dimensional ordered subsets expectation maximum (3D OSEM) algorithm without correction for attenuation or scatter. The region of interest was drawn manually in well-delineated liver and used to assess the kinetics of ^{18}F-FDG in the liver at an Inveon Research WorkStation. Hepatic uptake of ^{18}F-FDG was quantitatively expressed using the standardized uptake value percentage injected dose per gram (%ID/g).

2.10. Western blot

Target cells were incubated with the indicated factors for the designated times and subjected to Western blot analysis. Whole-cell lysates were extracted using Blue Loading Buffer Pack (Cell Signaling Technology, Danvers, MA, USA, 7722S) containing 1 mmol/L phenylmethylsulfonyl fluoride (PMSF). Fifty micrograms of mouse liver tissue was homogenized and lysed in RIPA buffer supplemented with 1 mmol/L PMSF to extract total protein. Protein concentrations were determined by BCA protein assay kit and all samples were diluted to the same concentration before denaturation. Sixty micrograms of protein was then subjected to sodium dodecyl sulfate-polyacrylamide gel electrophoresis (SDS-PAGE) separation, transferred onto a nitrocellulose membrane (NC) membrane by wet transfer (200 mA, 90 min), and incubated with primary antibodies followed by horseradish peroxidase (HRP)-conjugated secondary antibodies (all primary and secondary antibodies are presented in Supporting Information Table S1). The immunoreactive bands were detected by ECL reagent (Vazyme Biotech, Nanjing, China) using a gel imaging system (Tanon 5200 Multi, Tanon Science & Technology, Shanghai, China). The intensity of the bands was analyzed using the Image J software (NIH, USA).

2.11. Co-immunoprecipitation

Primary hepatocytes were cultured in Williams' Medium E containing PCN (10 μmol/L) for 48 h. The cultured cells were scraped in IP lysis buffer containing protease inhibitors. One milligram of protein extract was incubated with 2 μg anti-PXR antibody, anti-PGC1α antibody, or normal mouse IgG overnight at 4 °C with continuous mixing. Forty microliters of protein A/G magnetic beads were added for 2 h at 4 °C. The immunoprecipitates were pelleted by a magnetic stand and washed with PBS containing 0.1% Tween 20. The pellets were then suspended in 1× loading buffer and subjected to Western blot assays.

2.12. Dual luciferase assay

A PGL4.10-M_*Slc2a2* promoter-luciferase reporter construct harboring 2.0 kb of the M_*Slc2a2* promoter sequence (−1910 to +114) and a pRL *Renilla* luciferase control reporter vector (pRL-TK) were constructed by Genomeditech. A dual-luciferase reporter gene assay was performed using the dual-luciferase reporter gene assay kit according to the manufacturer's instruction, as follows. The mouse embryonic fibroblast cell line (NIH/3T3) from Cellcook Biotech (Guangzhou, China) was seeded in 24-well plates. After 12 h incubation, 0.2 μg/well PGL4.10-M_*Slc2a2* promoter-luciferase reporter and 0.2 μg/well pRL-TK were transfected into cells together with *Hnf4α* plasmid (50−200 ng/well). To transfect fixed amounts of DNA, sample DNA was supplemented with pEX-3 vector. For the luciferase assay in mouse primary hepatocytes, cells were transfected with luciferase reporters together with the siRNA target *Hnf4α* or treated with PCN. Luciferase activity was measured 48 h post-transfection of the NIH/3T3 cells. A *Renilla* luciferase internal control was used to normalize the relative luciferase activity.

2.13. Chromatin immunoprecipitation (ChIP) analysis

ChIP experiments were performed using the EZ-Magna ChIP kit according to the manufacturer's instructions. Briefly, primary hepatocytes in a 150 mm culture dish were treated with vehicle or PCN for 48 h and fixed by adding formaldehyde to the medium. Cells were harvested with lysis buffer and nuclear lysates were sonicated to yield DNA fragments of 0.2−1 kb. IP was performed using antibody to HNF4α (ab181604; Abcam, Cambridge, UK) or rabbit IgG. The purified DNA was amplified by real-time PCR. The primers used in the ChIP assays are as follows: *Glut2* gene's promoter was 5′-TCCTTCCGACCTTCATGTTC-3′ and 5′-GCTGTGCATTGGAGACTCAC-3′.

2.14. qRT-PCR

Total RNA was extracted from tissues or cells using RNAiso Plus Reagent and reverse-transcribed into cDNA using HiScript® III RT SuperMix (Vazyme). One microgram of RNA was incubated with 4× gDNA wiper mix at 42 °C for 2 min to remove genomic DNA, then 5× HiScript III qRT SuperMix was added to the reaction and incubated at 37 °C for 15 min, 85 °C for 5 s to synthesize cDNA. Gene expression analyses were performed with a CFX96 Real-Time PCR System (CFX96, Bio-Rad, USA) and ChamQ Universal SYBR qPCR Master Mix (Vazyme). The sequences of the mouse and human primers are presented in Supporting Information Table S2. The RNA levels of the target genes were normalized against the *ACTB* control levels using the comparative C_T ($\Delta\Delta C_T$) method.

2.15. Immunofluorescence assay

HepG2 cells were incubated with atorvastatin (10 μmol/L). Twenty-four hours later, cells were fixed with 4% formaldehyde for 15 min at room temperature. The cells were then blocked with 5% normal goat serum in PBS. After that, cells were incubated with primary antibody including GLUT2 (1:500) and Laminin

(1:1000) at 4 °C overnight. After triple washing with PBS, cells were further incubated with Alexa Fluor® 488- or 594-conjugated secondary antibody for 1 h at ambient temperature. The nucleus was stained with 4′,6-diamidino-2-phenylindole (DAPI). Finally, the cells were observed under a Cytation 5 Cell Imaging Multi-Mode Reader (BioTek, Germany) and images were processed using Gen 5 software.

2.16. Statistical analysis

All data are expressed as the mean ± standard deviation (SD). Comparisons between two groups were analyzed using unpaired Student's *t*-test. Multiple groups were compared using one-way ANOVA with Tukey's *post hoc* test. Correlation was assessed using the Pearson correlation analysis. Significant differences were accepted at $P < 0.05$. All statistical analyses were performed using GraphPad Prism 8.0 (GraphPad, La Jolla, CA, USA).

3. Results

3.1. PXR activation impaired glucose metabolism and downregulated expression of HNF4α and GLUT2 in HepG2 cells

The effects of the PXR agonists atorvastatin and rifampicin on glucose utilization, glucose uptake, and expression of GLUT2 and GCK in HepG2 cells were characterized. Consistent with a previous report[14], atorvastatin and rifampicin dose-dependently inhibited glucose utilization, glucose uptake, and the protein expression of GCK and GLUT2 (Fig. 1A, B, D–F). Expression of possible transcription factors or nuclear receptors related to GLUT2 and GCK expression such as nuclear receptor subfamily 4 group A member 1 (*NR4A1*), kruppel-like factor 7 (*KLF7*), peroxisome proliferator-activated receptor gamma (*PPARγ*), forkhead-box A3 (*FOXA3*), hypoxia-inducible factor 1 subunit alpha (*HIF1α*), sterol regulatory element binding transcription factor 1 (*SREBF1*), *PGC1α*, *HNF6*, *HNF4α*, *HNF1α*, and *HNF3β* were simultaneously measured using qRT-PCR. The results show that both atorvastatin and rifampicin significantly reduced gene expression of *HNF4α* and *GLUT2* but strongly induced gene expression of *PGC1α* (Fig. 1C). Similar to a previous report[37], *GCK* mRNA was undetectable in HepG2 cells. Protein expression of HNF4α was further analyzed. Both atorvastatin and rifampicin decreased protein expression of HNF4α (Fig. 1G and H) in a concentration-dependent manner. The downregulation of HNF4α expression was in parallel with the impairment of glucose utilization/uptake and expression of GLUT2 and GCK, indicating that the impaired hepatic glucose metabolism by PXR activation was possibly attributed to the downregulation of HNF4α expression. Both atorvastatin and rifampicin are strong PXR activators, whose inductive effects on cytochrome P450 3A4 (CYP3A4) are similar[38]. The present study also shows that the inhibitory effects of atorvastatin on hepatic glucose utilization/uptake and expression of GLUT2, GCK, and HNF4α protein are stronger than those of rifampicin. Thus, atorvastatin served as representative to further investigate the implications of PXR activation in impairment of hepatic glucose metabolism. An immunofluorescence assay also showed that atorvastatin remarkably decreased expression and distribution of GLUT2 on the plasma membrane (Fig. 1N). The role of PXR in the regulation of HNF4α expression was confirmed in *PXR*-silenced and PXR-overexpressing HepG2 cells. This was consistent with our expectation that silencing *PXR* would upregulate the expression of HNF4α and GLUT2, while overexpression of PXR would downregulate the expression of HNF4α and GLUT2 (Fig. 1I and J). It was also consistent with altered expression of GLUT2 that silencing *PXR* tended to increase glucose uptake, although no statistical significance was obtained. In contrast, overexpression of PXR markedly decreased glucose uptake (Fig. 1K). More importantly, atorvastatin no longer influenced the expression of GLUT2 and HNF4α in *PXR*-silenced HepG2 cells (Fig. 1L and M). These results further confirmed that PXR activation suppresses expression of HNF4α and GLUT2.

3.2. Importance of HNF4α in GLUT2 expression and glucose uptake in HepG2 cells

The importance of HNF4α in the regulation of GLUT2 and GCK expression and glucose metabolism was documented in both *HNF4α*-silenced and HNF4α-overexpressing HepG2 cells. The results show that silencing *HNF4α* significantly reduces expression of GLUT2, glucose uptake and glucose utilization (Fig. 2A–D). In contrast, overexpression of HNF4α remarkably increased the expression of GLUT2 (Fig. 2E and F) and glucose uptake (Fig. 2I). However, both silencing *HNF4α* and overexpressing HNF4α had little effect on the expression of GCK. Furthermore, overexpression of HNF4α also reversed the impairment of GLUT2 expression and glucose uptake induced by atorvastatin (Fig. 2G–I). The results indicate that HNF4α upregulated expression of GLUT2, and in turn, enhanced glucose uptake.

3.3. Importance of PXR and HNF4α in GLUT2 expression in human primary hepatocytes

The effects of atorvastatin on mRNA expression of *GLUT2, GCK*, and *HNF4α* in human primary hepatocytes from nine donors were also documented (Supporting Information Fig. S1D–S1L). *CYP3A4* served as a control gene. Results were consistent with the findings in HepG2 cells that atorvastatin significantly decreased mRNA expression of *GLUT2* and *HNF4α* in cells from 5 out of 9 donors. Correlation analysis showed that decreases in mRNA expression of *HNF4α*, *GLUT2*, and *GCK* by atorvastatin were positively correlated with the basal mRNA expression of *PXR*. However, the altered expression of *HNF4α*, *GLUT2*, and *GCK* mRNA were not related to induction of *CYP3A4* mRNA (Fig. 2J and Supporting Information Fig. S2). Furthermore, levels of *GLUT2* mRNA were positively correlated with *HNF4α* mRNA in atorvastatin-treated hepatocytes (Fig. 2K). We further investigated whether atorvastatin-induced downregulation of *HNF4α* and *GLUT2* was dependent on PXR using human primary hepatocytes from 3 donors. The results show that silencing *PXR* remarkably reversed the decreased expression of both *GLUT2* and *HNF4α* mRNA (Fig. 2L–N), as well as the induction of *CYP3A4* mRNA (Fig. S1A–S1C) in human primary hepatocytes. Moreover, silencing *HNF4α* also remarkably downregulated mRNA expression of *GLUT2* (Fig. 2O–Q). Although atorvastatin affected mRNA expression of *GCK*, the results were contradictory. In 5 out of 9 donors, atorvastatin significantly decreased mRNA expression of *GCK*, but in another 4 donors, atorvastatin significantly increased mRNA expression of *GCK*. Silencing *PXR* reversed the decreased mRNA expression of *GCK* in

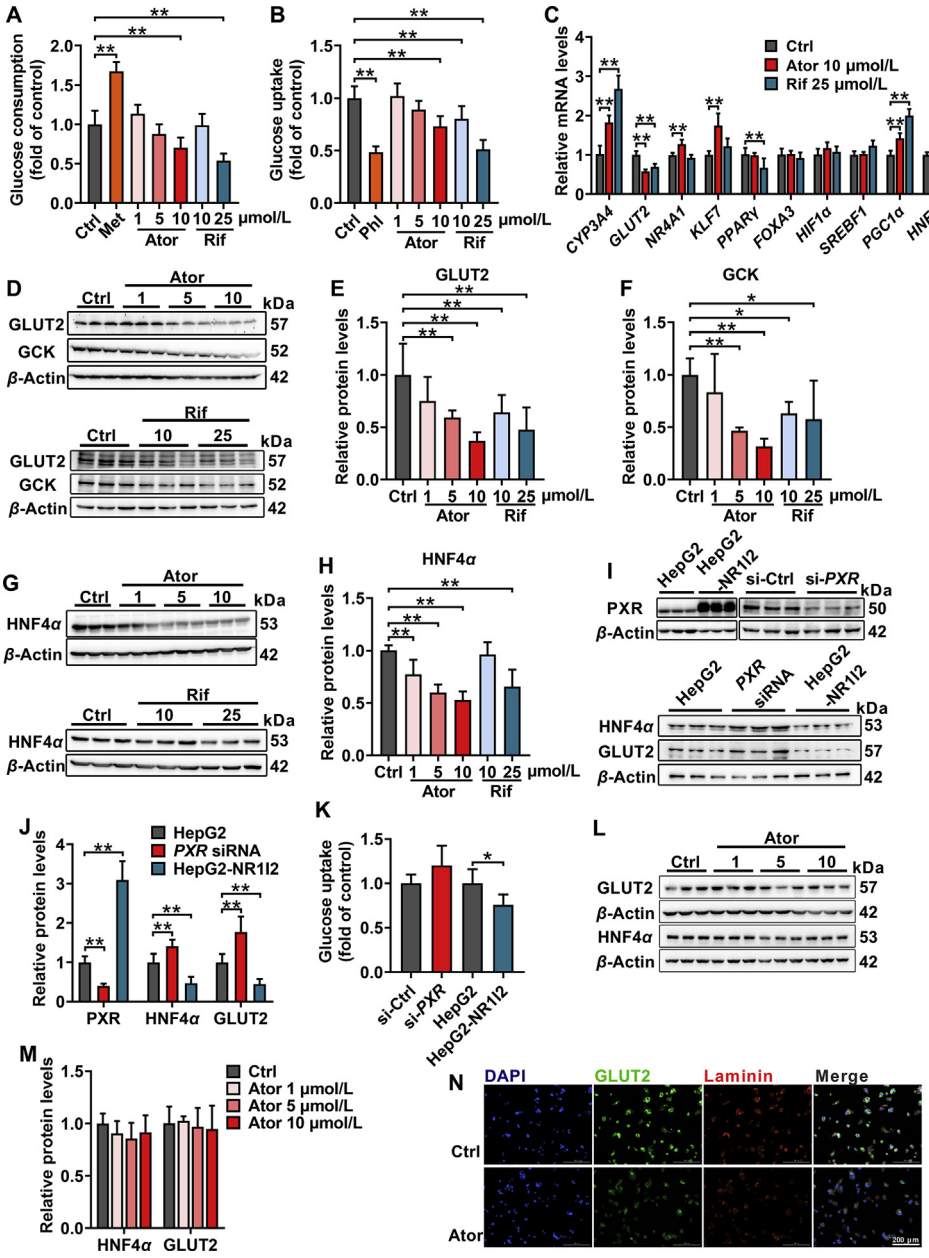

Figure 1 Effects of PXR activation on glucose metabolism and expression of HNF4α, GLUT2, and GCK in HepG2 cells. (A)–(C) Effects of atorvastatin and rifampicin on glucose consumption (A) and glucose uptake (B) as well as mRNA (C) expression of *CYP3A4*, *GLUT2*, *NR4A1*, *KLF7*, *PPARγ*, *FOXA3*, *HIF1α*, *SREBF1*, *PGC1α*, *HNF6*, *HNF4α*, *HNF1α*, and *HNF3β* in HepG2 cells. (D)–(F) Effects of atorvastatin and rifampicin on protein expression of GLUT2 and GCK in HepG2 cells. (G) and (H) Effects of atorvastatin and rifampicin on protein expression of HNF4α in HepG2 cells. (I) and (J) Expression of PXR, HNF4α, and GLUT2 in *PXR*-silenced and PXR-overexpressing HepG2 cells. (K) Glucose uptake in *PXR*-silenced and PXR-overexpressing HepG2 cells. (L) and (M) Effects of atorvastatin on protein expression of GLUT2 and HNF4α in *PXR*-silenced HepG2 cells. (N) Effects of atorvastatin on expression of membrane GLUT2 in HepG2 cells using immunofluorescence imaging. Data are represented as mean ± SD ($n = 6$). $^{*}P < 0.05$, $^{**}P < 0.01$. Ator, atorvastatin; Rif, rifampicin; Met, metformin; Phl, phloretin.

only 2 out of 3 donors. Similarly, silencing *HNF4α* downregulated expression of *GCK* mRNA in only 2 out of 3 donors.

3.4. *PXR activation impaired glucose uptake by inhibiting the HNF4A–GLUT2 pathway in mouse primary hepatocytes*

PCN and *Cyp3a11* served as mouse PXR agonist and control gene, respectively. PCN significantly induced mRNA expression of *Cyp3a11*, demonstrating PXR activation in mouse primary hepatocytes by PCN (Fig. 3A and E). The effects of incubation time with PCN on mRNA expression of *Glut2* and *Gck* showed that 24 h incubation with PCN exhibited stronger inhibitory effects on mRNA expression of *Glut2* and *Gck* than 12 h incubation (Fig. 3A). In general, alterations in target proteins and their functions lag behind the altered expression of their mRNA. Both 24 and 48 h incubations were further selected to investigate effects of PCN on protein expressions of GLUT2 and GCK as well as glucose uptake in mouse primary hepatocytes. The results show

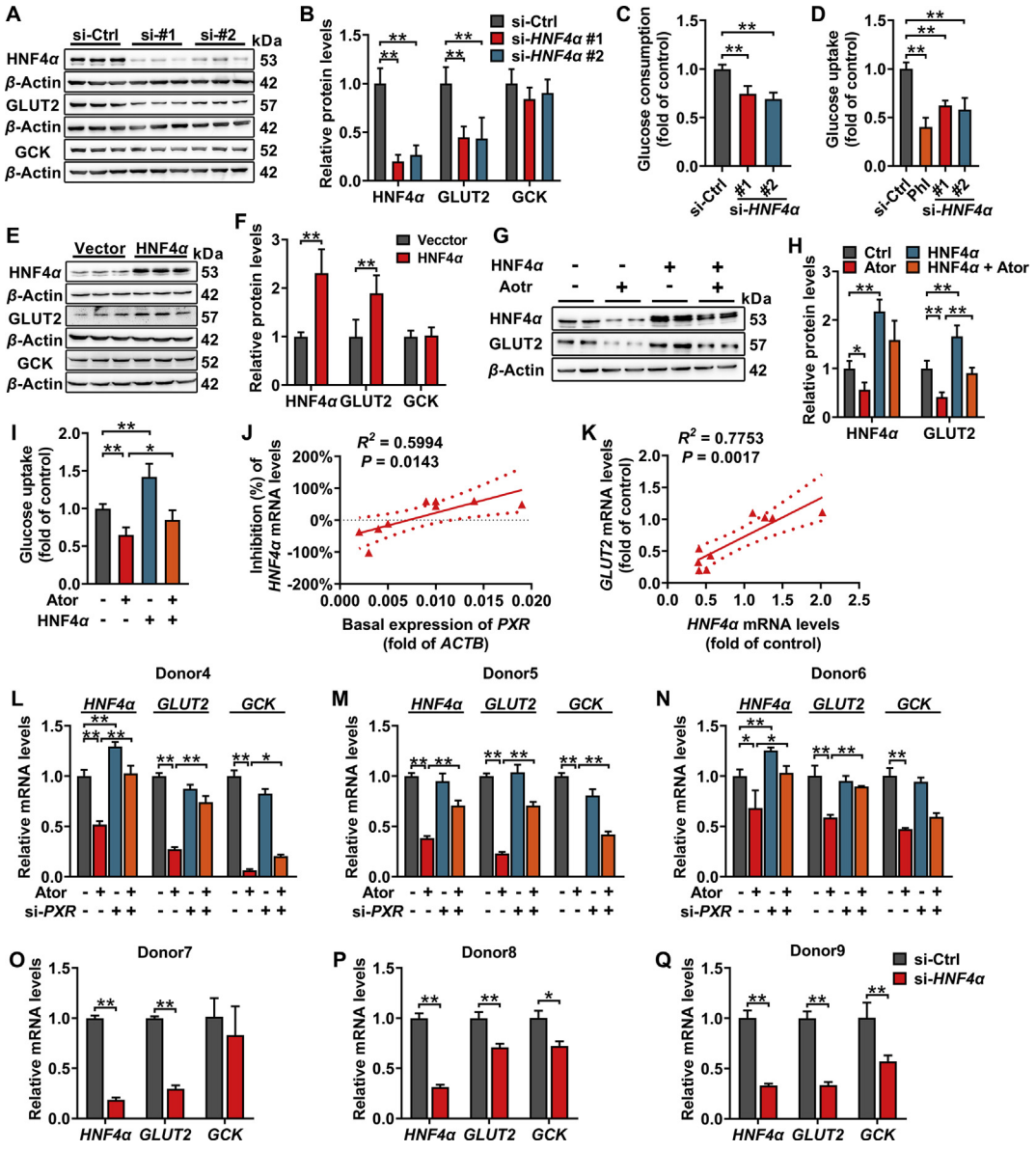

Figure 2 HNF4α promotes the expression of GLUT2 and glucose uptake in HepG2 cells and PXR activation downregulates expression of *HNF4α* and *GLUT2* in human primary hepatocytes. (A)−(D) Protein expression of HNF4α, GLUT2, and GCK (A, B), and glucose consumption (C) and glucose uptake (D) in *HNF4α*-silenced HepG2 cells ($n = 6$). (E) and (F) Protein expression of HNF4α, GLUT2, and GCK in HNF4α-overexpressing HepG2 cells ($n = 6$). (G)−(I) Protein expression of GLUT2 and HNF4α (G, H) and glucose uptake (I) in atorvastatin-treated HepG2 cells or HNF4α-overexpressing HepG2 cells ($n = 6$). (J) Correlation between basal mRNA levels of *PXR* and percent inhibition of *HNF4α* mRNA expression in atorvastatin-treated human primary hepatocytes from nine different donors ($n = 9$). Basal *PXR* expression is given as the ratio of *PXR* mRNA to *ACTB* mRNA in the control group. (K) Positive relationship between altered mRNA expression of *HNF4α* and *GLUT2* in atorvastatin-treated human primary hepatocytes from nine different donors ($n = 9$). (L)–(N) Effects of silencing *PXR* on mRNA levels of *HNF4α, GLUT2, and GCK* in atorvastatin-treated human primary hepatocytes ($n = 3$). (O)−(Q) Effects of silencing *HNF4α* on mRNA levels of *GLUT2 and GCK* in human primary hepatocytes ($n = 3$). Data are represented as mean ± SD. $^{*}P < 0.05$, $^{**}P < 0.01$.

that PCN time-dependently decreased the protein expression of GLUT2 (Fig. 3B and C) and impaired glucose uptake (Fig. 3D). Meanwhile, PCN also downregulated mRNA and protein expressions of HNF4α and GLUT2 (Fig. 3E–G) in a concentration-dependent manner, which was in line with a decrease in glucose uptake (Fig. 3H). This is similar to the findings with HepG2 cells that silencing *Pxr* also reverses the downregulated protein expression of HNF4α and GLUT2, and the impairment of glucose uptake by PCN (Fig. 3I–K). Although PCN also significantly downregulated the mRNA expression of *Gck*, the protein level of GCK was only slightly suppressed with no statistical significance. The mRNA expression of *Pck1* and *G6pc* were altered in opposite directions (Supporting Information Fig. S3C and S3D). Moreover, PXR activation did not affect glucose production in mouse primary hepatocytes (Fig. S3E).

To determine whether HNF4α directly regulated GLUT2 expression, *Hnf4α* was silenced in mouse primary hepatocytes using two separate *Hnf4α* siRNAs; scrambled siRNA served as a

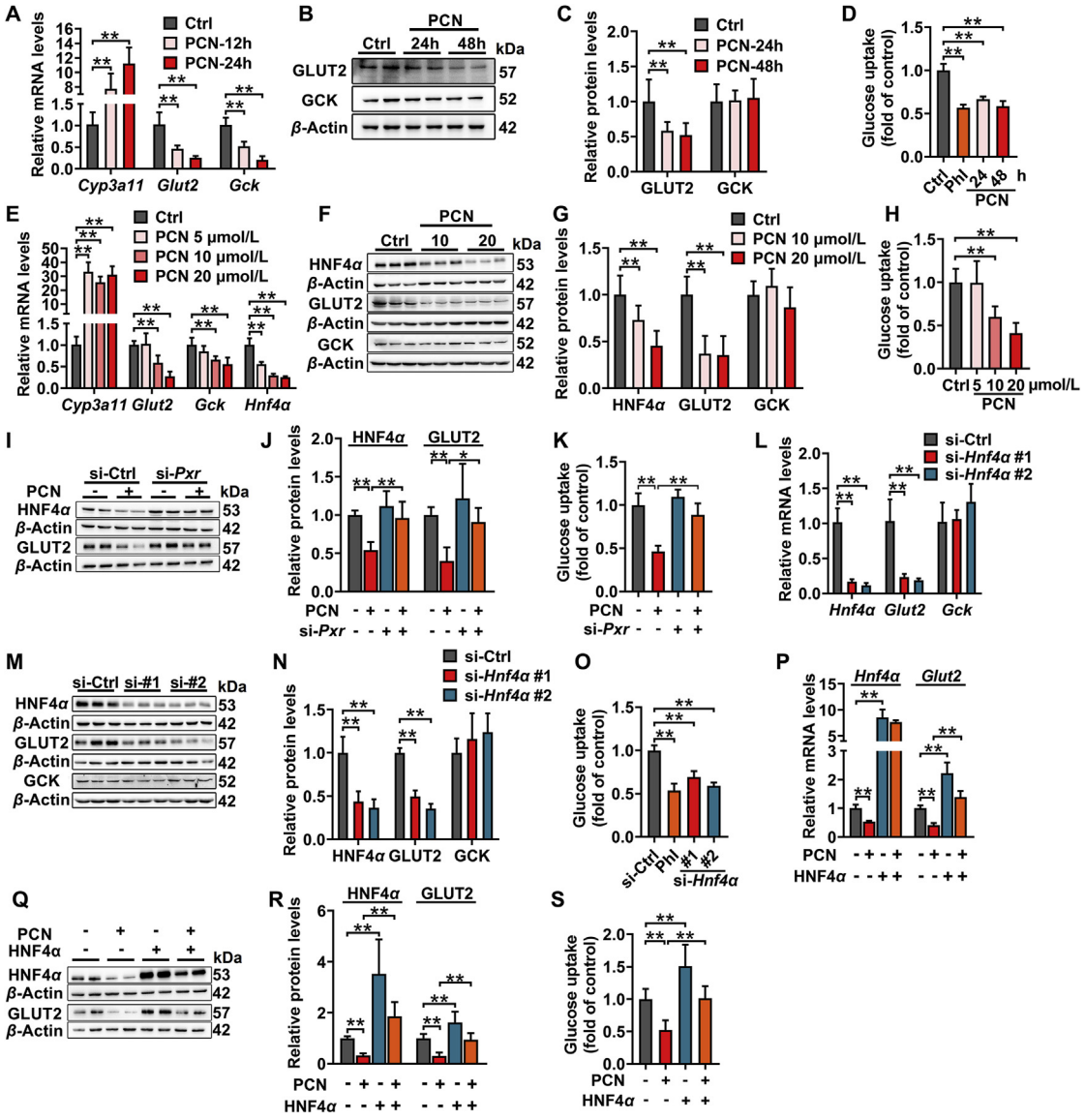

Figure 3 Activation of PXR impairs glucose uptake by inhibiting the HNF4α−GLUT2 pathway in mouse primary hepatocytes. Effects of 12 and 24 h PCN (10 μmol/L) treatment on the mRNA (A) and protein (B and C) expression of GLUT2 and GCK as well as glucose uptake (D) in mouse primary hepatocytes. Effects of different concentrations of PCN on the mRNA (E) and protein (F and G) expression of HNF4α, GLUT2, and GCK as well as glucose uptake (H) in mouse primary hepatocytes. Effects of *Pxr* silencing on impaired protein (I and J) expression of HNF4α and GLUT2 as well as glucose uptake (K) by PCN in mouse primary hepatocytes. Effects of *Hnf4α* silencing on the mRNA (L) and protein (M and N) expression of GLUT2 and GCK as well as glucose uptake (O) in mouse primary hepatocytes. Effects of HNF4α overexpression on impaired mRNA (P) and protein (Q and R) expression of GLUT2 as well as glucose uptake (S) by PCN. Data are represented as mean ± SD ($n = 6$). $^{*}P < 0.05$, $^{**}P < 0.01$.

control (Fig. 3L–O). The results show that the mRNA and protein expression of HNF4α in cells transfected with two separate *Hnf4α* siRNAs was significantly decreased to 11% and 36% of control cells, respectively, indicating a successful silencing of *Hnf4α*. This was consistent with our expectation that silencing *Hnf4α* would significantly downregulate mRNA and protein expression of GLUT2 and impair glucose uptake without affecting the expression of GCK. In contrast, overexpression of HNF4α upregulated mRNA (Fig. 3P) and protein (Fig. 3Q and R) expression of GLUT2 and promoted glucose uptake (Fig. 3S). More importantly, overexpressing HNF4α abolished downregulation of GLUT2 at both the mRNA and the protein levels (Fig. 3P–R), and the impairment of glucose uptake (Fig. 3S) induced by PCN. These results further demonstrate that *Glut2* is a target gene of HNF4α and that PXR activation downregulates expression of GLUT2 by decreasing HNF4α expression, and in turn, impairing glucose uptake.

3.5. HNF4α, as a transactivation factor, directly bound to the Slc2a2 promoter and PXR activation disrupted the binding of HNF4α to the Slc2a2 promoter

NIH/3T3 cells are commonly used in dual-luciferase reporter gene assays. More importantly, NIH/3T3 cells do not express GLUT2

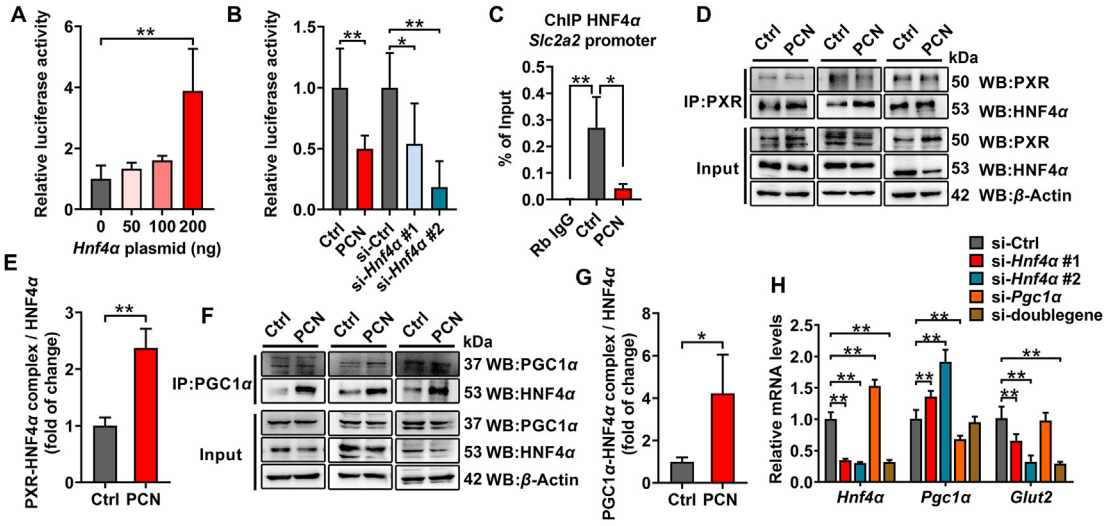

Figure 4 Association of HNF4α with transcriptional activation of GLUT2 and effects of PXR activation by PCN on the formation of the PXR−HNF4α complex and the HNF4α−PGC1α complex. (A) HNF4α dose-dependently activated the *Slc2a2* promoter in NIH/3T3 cells ($n = 6$). (B) Relative *Slc2a2* promoter luciferase reporter activity in mouse primary hepatocytes treated with PCN (10 μmol/L) or silenced *Hnf4α* for 48 h. The luciferase activity generated was normalized by a co-transfected internal pRL-TK control plasmid expressing *Renilla* luciferase ($n = 6$). (C) ChIP analysis for HNF4α binding on the *Slc2a2* promoter followed by qRT-PCR in mouse primary hepatocytes treated with PCN (10 μmol/L) for 48 h ($n = 3$). (D)–(G) PXR activation by PCN increased the formation of the PXR–HNF4α complex and the HNF4α–PGC1α complex in mouse primary hepatocytes. Western blot analysis with the indicated antibodies in total cell lysates and precipitates after immunoprecipitation with anti-PXR antibody (D) or anti-PGC1α antibody (F). The quantitative data were indexed as the ratio of HNF4α complex to total HNF4α (E and G; $n = 3$). (H) Effects of both silencing *Hnf4α* and *Pgc1α* on the expression of *Glut2* in mouse primary hepatocytes ($n = 6$). Data are represented as mean ± SD. $^{*}P < 0.05$, $^{**}P < 0.01$.

and HNF4α. Here, NIH/3T3 served as a cell model to determine whether HNF4α activates the *Glut2* promoter. NIH/3T3 cells were simultaneously transfected with the PGL4.10-M_*Slc2a2* promoter-luciferase reporter construct and different doses of *Hnf4α* plasmid (50, 100, and 200 ng). The *Hnf4α* plasmid increased *Slc2a2* promoter-luciferase reporter activity in a dose-dependent manner (Fig. 4A). Mouse primary hepatocytes were transfected with a PGL4.10-M_*Slc2a2* promoter-luciferase reporter construct and simultaneously transfected with *Hnf4α* siRNA. The results show that both *Hnf4α* silencing and PCN significantly suppressed *Slc2a2* promoter activity (Fig. 4B) to 15% and 50% of control cells, respectively.

To further confirm whether HNF4α directly bound to the *Slc2a2* promoter, ChIP assays were performed in mouse primary hepatocytes. IgG served as a negative control. Results from three independent experiments show that the levels of HNF4α antibody binding to *Slc2a2* promoter were much greater than that of IgG, demonstrating direct binding of HNF4α to the *Slc2a2* promoter. PCN significantly reduced the recruitment of HNF4α on the *Slc2a2* promoter (Fig. 4C). These results demonstrate that HNF4α is a transactivation factor of *Slc2a2* and that PXR activation disrupts the binding of HNF4α to *Slc2a2* promoter.

3.6. *Roles of PXR–HNF4α complex and HNF4α–PGC1α complex in regulation of GLUT2 expression upon PXR activation*

PGC1α has been widely investigated as an interacting coactivator regulating liver energy metabolism[39]. PGC1α cross-talks with HNF4α in the form of a complex and then promotes the transcriptional activity of HNF4α in the regulation of downstream genes[40,41]. A co-immunoprecipitation assay was conducted with mouse primary hepatocytes to investigate the roles of the PXR–HNF4α complex and the HNF4α–PGC1α complex in transcriptional regulation of *Glut2* expression upon PXR activation (Fig. 4D–G). The results indicate that PXR activation by PCN significantly increased formation of a PXR–HNF4α complex (Fig. 4D and E) and a HNF4α–PGC1α complex (Fig. 4F and G). The role of PGC1α in the regulation of *Glut2* expression by HNF4α was also documented in mouse primary hepatocytes using *Pgc1α* siRNA. In contrast to our expectation, *Pgc1α* silencing little affected expression of *Glut2*. Moreover, simultaneously silencing *Pgc1α* and *Hnf4α* showed no synergistic effect, indicating that HNF4α-mediated transcriptional regulation of *Glut2* was not affected by PGC1α (Fig. 4H).

3.7. *PXR activation impaired glucose metabolism in the livers of mice possibly by inhibiting the HNF4α–GLUT2 pathway*

Our *in vitro* data showed that PXR activation impairs glucose metabolism possibly by inhibiting the HNF4α–GLUT2 pathway. Mouse experiments were performed to confirm this *in vitro* data using the typical PXR activator PCN (Table 1; Fig. 5). The results show that compared with vehicle-control mice, 5-day PCN treatment significantly impairs glucose tolerance, leading to increases in plasma glucose levels and area under the curve $(AUC)_{0-90\ min}$ values (Fig. 5A and B) during IPGTT, although fasting glucose levels were unaltered. PCN also significantly downregulated mRNA and protein expression of GLUT2 and HNF4α in mouse liver (Fig. 5C–E), where these proteins were decreased to 47% and 57% of control mice, respectively. However, PCN did not affect the hepatic expression of GCK protein, although a significant decrease was observed in the expression of *Gck* mRNA (Fig. 5C–E). Moreover, the liver weight (6.0% ± 1.0% of body weight) of mice treated with PCN was significantly higher than

Table 1 Physiological and biochemical parameters in mice.

Parameter	Ctrl	PCN	AAV8-Ctrl	AAV8-*Hnf4α*-shRNA
Body weight (g)	19.3 ± 1.1	18.9 ± 0.9	21.6 ± 1.5	20.8 ± 0.8
Liver weight (% of body weight)	4.3 ± 0.5	6.0 ± 1.0**	3.9 ± 0.1	4.9 ± 0.5**
FPG (mmol/L)	5.5 ± 0.7	5.2 ± 1.1	7.0 ± 0.3	6.8 ± 1.2
FINS (ng/mL)	0.61 ± 0.34	0.83 ± 0.44	0.48 ± 0.19	1.07 ± 0.42*
HOMA-IR	3.15 ± 1.76	4.18 ± 2.44	3.13 ± 1.30	7.18 ± 3.77*
Liver glycogen (mg/g liver)	6.81 ± 4.03	4.98 ± 2.37	3.34 ± 2.32	2.45 ± 0.63
Plasma AST (U/L)	24.63 ± 3.76	33.08 ± 14.97	29.20 ± 7.83	26.83 ± 9.61
Plasma ALT (U/L)	11.37 ± 3.23	21.07 ± 8.45*	11.40 ± 3.30	11.42 ± 6.23
Plasma AKP (U/L)	19.30 ± 6.85	21.70 ± 8.29	21.62 ± 1.12	17.99 ± 4.67

Data are represented as mean ± SD (n = 5−6 mice). Ctrl, control mice; PCN, PCN-treated mice; AAV8-Ctrl, mice injected with AAV8-vectors; AAV8-*Hnf4α*-shRNA, mice injected with AAV8-*Hnf4α*-shRNA. FPG, fasting plasma glucose; FINS, fasting plasma insulin; AST, aspartate aminotransferase; ALT, alanine aminotransferase; AKP, alkaline phosphatase. $^{*}P < 0.05$, $^{**}P < 0.01$ *versus* control group.

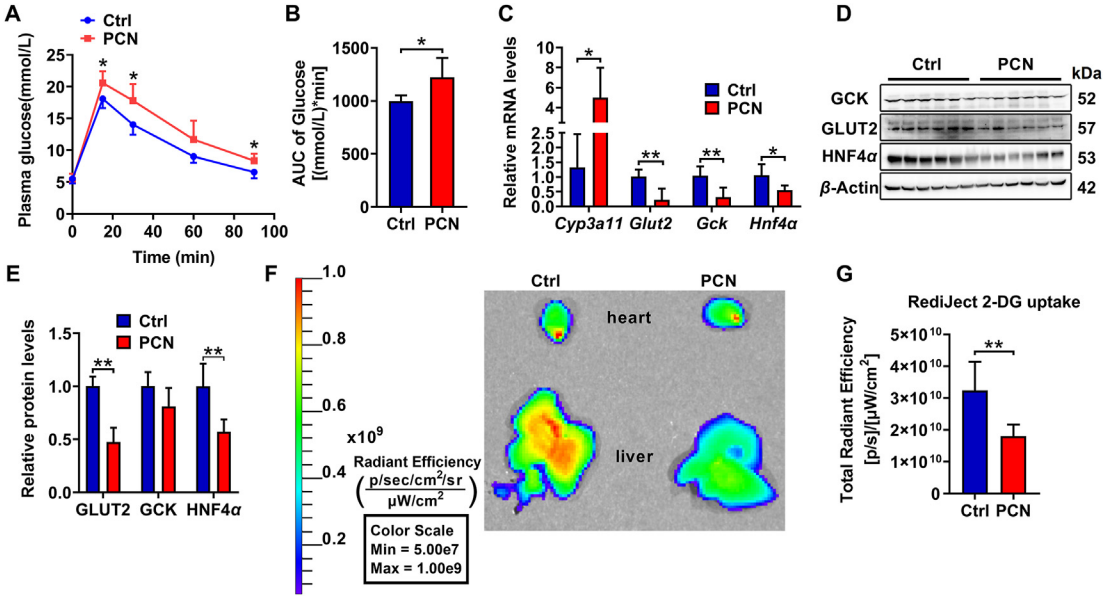

Figure 5 5-Day PCN treatment impairs glucose tolerance and hepatic glucose uptake in C57BL/6J mice. Effects of 5-day PCN treatment on glucose levels after intraperitoneal injection of 2 g/kg glucose (A). Quantitation of glucose area under the curve is shown in (B). Effects of 5-day PCN treatment on the mRNA (C) and protein (D and E) expression of CYP3A11, GLUT2, GCK, and HNF4α in mouse liver. (F and G) Effects of 5-day PCN treatment on uptake of RediJect-2DG in liver. Data are represented as mean ± SD (n = 6). $^{*}P < 0.05$, $^{**}P < 0.01$ *versus* control mice.

that (4.3% ± 0.5% of body weight) of control mice ($P < 0.01$; Table 1). PCN showed a trend to increase fasting insulin levels, but no statistical significance was observed.

To determine whether the PCN-induced GLUT2 supression contributed to impairment of hepatic glucose uptake, *in vivo* hepatic glucose uptake in mice was measured using RediJect 2-DG-750 as a probe. Results were consistent with downregulation of hepatic GLUT2 expression that PCN treatment significantly decreased hepatic glucose uptake to 55% of that in control mice (Fig. 5F and G). These data support the hypothesis that PCN impairs hepatic glucose uptake partly by downregulating GLUT2 expression.

3.8. Liver-specific knockdown of Hnf4α gene impaired glucose metabolism by impairing GLUT2-mediated hepatic glucose uptake in mice

To further investigate the importance of HNF4α in hepatic glucose metabolism *in vivo*, liver-specific *Hnf4α* knockdown C57BL/6J mice were developed using AAV8-shRNA by intraportal vein injection (Fig. 6). Fluorescence imaging demonstrated liver-specific gene expression (Supporting Information Fig. S4). qRT-PCR and Western blot analyses also demonstrated that liver-specific knockdown remarkably lowered mRNA (Fig. 6H) and protein (Fig. 6I and J) expression of HNF4α in mouse liver, which was only 34% and 28% of control mice, respectively, confirming that the *Hnf4α* gene was silenced. IPGTT data shows that *Hnf4α* silencing significantly elevated plasma glucose levels, whose $AUC_{0-90\ min}$ was increased by 30% of control mice (Fig. 6D and E), although fasting glucose levels were unaltered. It was also found that liver *Hnf4α* knockdown mice showed remarkably higher fasting insulin levels (1.07 ± 0.42 ng/mL *versus* 0.48 ± 0.19 ng/mL in control mice, $P < 0.05$). The effects of liver-specific *Hnf4α* knockdown on insulin secretion were further documented during an oral glucose dose. The results show that *Hnf4α* silencing elevated plasma glucose levels (Fig. 6F) and showed a trend to promote insulin release (Fig. 6G) during OGTT; statistical significance was obtained at 15 min following the glucose dose.

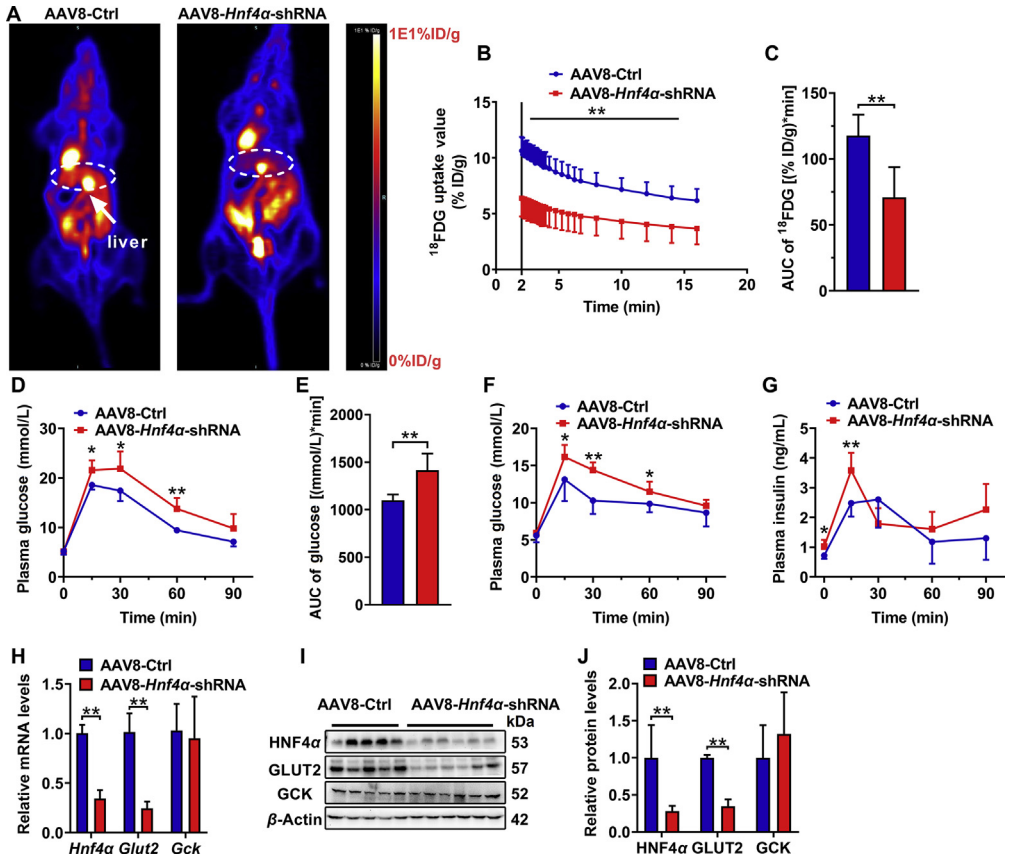

Figure 6 Absence of liver HNF4α expression impairs glucose tolerance and hepatic glucose uptake in C57BL/6J mice. PET/CT imaging (A) and kinetics (B) of ^{18}F-FDG uptake by the livers of control mice and liver-specific *Hnf4α* knockdown mice. Quantitation of ^{18}F-FDG area under the curve shown in (C) ($n = 6$). (D) Effects of liver-specific *Hnf4α* silencing on glucose levels after intraperitoneal injection of 2 g/kg glucose. Quantitation of glucose area under the curve is shown in (E) ($n = 5-6$). Effects of liver-specific *Hnf4α* silencing on plasma glucose (F) and insulin (G) levels during an oral glucose tolerance test ($n = 6$). Effects of liver-specific *Hnf4α* silencing on mRNA (H) and protein levels (I and J) of HNF4α, GLUT2, and GCK in mouse liver ($n = 5-6$). Data are represented as mean ± SD. $^{*}P < 0.05$, $^{**}P < 0.01$ *versus* control mice.

Expression of target proteins were also measured. It was in line with the altered expression of HNF4α that hepatic *Hnf4α* knockdown significantly lowered mRNA (Fig. 6H) and protein (Fig. 6I and J) expression of GLUT2 in the livers of mice, which were decreased to 24% and 45% of control mice, respectively. However, *Hnf4α* silencing little affected mRNA (Fig. 6H) and protein (Fig. 6I and J) expression of GCK. Similar to findings with PCN-treated mice, *Hnf4α* silencing also significantly increased liver weight from 3.9% ± 0.1% of body weight in control mice to 4.9% ± 0.5% of body weight in *Hnf4α* knockdown mice ($P < 0.01$; Table 1).

PET/CT imaging of ^{18}F-FDG was further used to measure hepatic glucose uptake. Consistent with the decrease in GLUT2 expression, the knockdown of the liver *Hnf4α* gene remarkably decreased ^{18}F-FDG uptake. The time course of ^{18}F-FDG accumulation in the livers of *Hnf4α* knockdown mice exhibited a remarkable decrease, where the $AUC_{2-16\ min}$ was only 60% of that of control mice (Fig. 6A–C), confirming impairment of hepatic glucose uptake.

4. Discussion

Accumulating evidence has demonstrated that PXR is involved in the regulation of hepatic glucose metabolism[16,29,42] and that PXR activation is strongly associated with an increased risk of hyperglycemia, even diabetes[29]. We reported that the rodent PXR activator PCN and atorvastatin impaired glucose tolerance in rats fed a high-fat diet, which was attributed to downregulations of hepatic GLUT2 and GCK expression[14]. PCN was also reported to impair glucose tolerance and downregulate expression of hepatic GLUT2 and GCK in wild-type mice but not in *Pxr* knockout mice[15]. In HepG2 cells, it was reported that the human PXR activators rifampicin and atorvastatin also impaired glucose metabolism and downregulated expression of GLUT2 and GCK[14]. These results indicate that PXR activation impairs glucose metabolism, possibly by downregulating GLUT2 and GCK expression. However, the molecular mechanisms by which PXR represses expression of GLUT2 and GCK have not been elucidated. This is the first report that PXR activation impairs glucose metabolism possibly by inhibiting the HNF4α–GLUT2 pathway. A series of experiments were designed to support the above hypothesis.

We firstly observed that HNF4α and GLUT2 were downregulated at both the mRNA and protein levels upon PXR activation. Expression of HNF4α and GLUT2 were strongly associated in *PXR*-silenced and PXR-overexpressing HepG2 cells. Overexpressing PXR downregulated, while silencing *PXR* upregulated expression of HNF4α and GLUT2. Moreover, silencing *PXR* prevented the atorvastatin-induced downregulation of

HNF4α and GLUT2. Similar results were obtained in primary hepatocytes from humans and mice. The extent of decrease in the mRNA levels of *HNF4α* and *GLUT2* with atorvastatin was strongly associated with the basal expression of *PXR*, indicating that the impairment of glucose metabolism by PXR is highly dependent on basal levels of *PXR* expression in human primary hepatocytes. Similarly, the atorvastatin-induced decrease in mRNA expression of *HNF4α* and *GLUT2* was dependent on PXR activation. PCN also downregulated mRNA and protein expression of HNF4α and GLUT2 as well as glucose uptake in mouse primary hepatocytes, which was reversed by silencing *Pxr*. These results suggest that PXR activation decreases the expression of GLUT2 by inhibiting the expression of HNF4α.

Next, we focused on the association of HNF4α with GLUT2. The data obtained in HepG2 cells were consistent with the results obtained with mouse primary hepatocytes. Silencing *HNF4α* decreased, but overexpressing HNF4α increased expression of GLUT2 without affecting expression of GCK. More importantly, overexpression of HNF4α abolished the downregulation of GLUT2 expression and impairment of glucose uptake induced by PXR activation. We further demonstrated that HNF4α directly bound to the *Glut2*/*Slc2a2* gene promoter and activated its transcription. PXR activation reduced recruitment of HNF4α on the *Slc2a2* promoter, resulting in *Slc2a2* transcriptional repression. The roles of HNF4α in regulating GLUT2 have also been demonstrated in other cells such as pancreatic β cells and embryonic stem cells[43,44]. These results lead to the conclusion that expression of hepatic GLUT2 is controlled by HNF4α and further confirm the importance of HNF4α downregulation by PXR activation in impairment of GLUT2 expression and glucose metabolism.

The importance of the PXR–HNF4α–GLUT2 pathway in impairment of hepatic glucose metabolism was further demonstrated in both PCN-treated mice and hepatic *Hnf4α* knockdown mice. As expected, PCN markedly reduced expression of both HNF4α and GLUT2. Data from IPGTT also demonstrated that PCN significantly impaired glucose tolerance. In line with the decreased expression of hepatic GLUT2, PCN also remarkably inhibited hepatic glucose uptake using RediJect 2-DG-750 as a probe. All these results demonstrate that PXR activation impaired GLUT2-mediated hepatic glucose uptake by downregulating HNF4α expression.

Liver-specific *Hnf4α* knockdown mice were developed using AAV8-shRNA to further confirm the role of HNF4α in hepatic glucose metabolism. Results were consistent with our expectation that liver-specific deletion of *Hnf4α* would significantly elevate plasma glucose levels during IPGTT. A PET/CT scan also showed that liver-specific *Hnf4α* knockdown remarkably decreased hepatic glucose uptake (^{18}F-FDG). Liver *Hnf4α* silencing impaired glucose tolerance and hepatic glucose uptake, which was in a good agreement with the downregulated expression of hepatic GLUT2 and HNF4α, and further confirming that HNF4α was implicated in GLUT2-mediated glucose uptake. All the above results argue strongly that PXR activation impairs hepatic glucose metabolism by inhibiting the HNF4α–GLUT2 pathway.

In addition to HNF4α, other hepatocyte nuclear factors such as HNF1α, HNF3β, and HNF6 have been demonstrated to regulate GLUT2 expression in previous studies[45,46]. Activated PXR often cross-talks with other nuclear factors. We screened other nuclear factors possibly related to expression of GLUT2 in HepG2 cells, and found that among the tested nuclear factors (*NR4A1*, *KLF7*, *PPARγ*, *FOXA3*, *HIF1α*, *SREBF1*, *PGC1α*, *HNF6*, *HNF4α*, *HNF1α*, *and HNF3β*), only expression of *HNF4α* and *GLUT2* mRNA were significantly suppressed by atorvastatin and rifampicin, although HNF1α, HNF3β, and HNF6 were also reported to regulate GLUT2 expression[45−47]. The effect of HNF1α on GLUT2 is tissue-specific. A report showed that HNF1α was essential for GLUT2 expression in differentiated β-cells but not in other tissues[48]. Reports on the effects of HNF3β on expression of GLUT2 are also conflicting. One report showed that HNF3β acted as a transcriptional activator of GLUT2[45], but the result was not reproduced in another study[47]. PGC1α, as a downstream sensor of metabolism, controls glucose-related gene transcription[39]. Our results show that silencing *Pgc1α* did not affect expression of *Glut2*, although both atorvastatin and rifampicin markedly induced gene expression of *PGC1α*. These results indicate the minor roles of HNF1α, HNF3β, HNF6, and PGC1α in downregulation of GLUT2 expression by PXR activation.

Other mechanisms also may be involved in the impairment of hepatic glucose metabolism by PXR activation. GCK, as a glucose sensor, plays a key role in postprandial glycemic control[49,50]. The basal mRNA expression of *Gck* was reduced by half in *PXR*-humanized (h*PXR*) transgenic mice compared to wild-type mice[51]. Data from HepG2 cells showed that, similarly to a previous report[14], PXR activation also significantly downregulated expression of GCK, indicating that downregulation of GCK expression is also a reason that PXR activation impairs glucose metabolism. However, in human primary hepatocytes atorvastatin downregulated the expression of *GCK* mRNA in only 5 out of the tested 9 donors. Silencing PXR also reversed the downregulation of *GCK* mRNA by atorvastatin in 2 out of 3 donors. In mouse primary hepatocytes, PCN little affected protein expression of GCK. These results indicate that the roles of GCK in impairment of hepatic glucose metabolism by PXR activation needs further investigation. HNF4α did not affect GCK expression in HepG2 cells, indicating that HNF4α was not involved in GCK-mediated impairment of glucose metabolism by PXR activation. Several studies have demonstrated a role for PXR activation in gluconeogenesis, but the results are contradictory. Earlier studies showed that PXR ligands inhibited the expression of gluconeogenic genes[30,52]. Gotoh et al.[53,54] reported that the PXR activators rifampicin and simvastatin induced the expression of PEPCK and G6Pase through serum- and glucocorticoid-regulated kinase 2 in HepG2 cells. However, our previous report showed that atorvastatin and rifampicin little affected glucose production and the protein expression of PEPCK and G6Pase in HepG2 cells[14]. In the study, we also found that PXR activation did not affect glucose production in mouse primary hepatocytes.

It is noteworthy that *Hnf4α* silencing and PXR activation resulted in obvious hepatomegaly. PXR activation induces liver enlargement[55]. Dexamethasone[4] and mifepristone[56] also induce hepatomegaly by activating PXR. HNF4α is critical for hepatic differentiation[57,58]. In mice, it was reported that hepatocyte-specific deletion of *Hnf4α* resulted in spontaneous hepatocyte proliferation[57] and increased mortality post partial hepatectomy[57,58]. And, a report showed the reciprocal negative regulation of HNF4α and cyclin D1, a key cell cycle protein in the liver. Hepatocyte cyclin D1 gene ablation caused markedly increased postprandial liver glycogen levels[59]. The PXR activator PCN also significantly downregulated protein expression of HNF4α, which also contributes to hepatomegaly.

We also noticed that liver-specific *Hnf4α* deletion increased levels of fasting plasma insulin. Further study showed that liver-specific *Hnf4α* deletion markedly increased insulin release by oral glucose loading, indicating that liver-specific *Hnf4α* deletion impairs glucose metabolism not by impairing insulin release. The

effects of liver-specific *Hnf4α* deletion on insulin release differed from data from β-cell *Hnf4α* deletion. β-Cell deletion of *Hnf4α* was reported to induce hyperinsulinemia but impair glucose tolerance and insulin release in mice[60]. However, another report showed that β-cell deletion of *Hnf4α* did not affect fasting blood glucose and insulin levels, although glucose tolerance and insulin release were impaired[61]. The reasons leading to these discrepancies need further investigation.

5. Conclusions

HNF4α is a transactivator of the *GLUT2* gene in hepatocytes. PXR activation impaired hepatic glucose metabolism partly by inhibiting the HNF4α–GLUT2 pathway. The results reveal the molecular mechanisms by which PXR activators induce hyperglycemia/diabetes.

Acknowledgments

This work was supported by the National Natural Science Foundation of China (Nos. 81673505, 81872930, and 82073922), the "Double First-Class" university project (No. CPU2018GY22, China), and "333" Project of Jiangsu Province (No. BRA2020287, China). We thank members of Key Laboratory of Nuclear Medicine of Nanjing First Hospital for providing technical assistance (Nanjing, China). We appreciate technical support by the Public Experimental Pharmacology Platform of China Pharmaceutical University (Nanjing, China).

Author contributions

Peihua Liu: conceptualization, methodology, investigation, data curation, validation, and writing-original draft. Li Liu and Xiaodong Liu: conceptualization, methodology, writing-reviewing, editing, and supervision. Jianjun Zou: conceptualization and software. Ling Jiang and Weimin Kong: investigation, validation, and data curation. Qiushi Xie, Ping Li, Xiaonan Liu, Jiayi Zhang, Ming Liu, Zhongjian Wang, Liang Zhu, Hanyu Yang, and Ying Zhou: investigation.

Conflicts of interest

The authors declare no conflicts of interest.

Appendix A. Supporting information

Supporting data to this article can be found online at https://doi.org/10.1016/j.apsb.2021.09.031.

References

1. Liu MZ, He HY, Luo JQ, He FZ, Chen ZR, Liu YP, et al. Drug-induced hyperglycaemia and diabetes: pharmacogenomics perspectives. *Arch Pharm Res* 2018;**41**:725−36.
2. Fathallah N, Slim R, Larif S, Hmouda H, Ben Salem C. Drug-induced hyperglycaemia and diabetes. *Drug Saf* 2015;**38**:1153−68.
3. Jain V, Patel RK, Kapadia Z, Galiveeti S, Banerji M, Hope L. Drugs and hyperglycemia: a practical guide. *Maturitas* 2017;**104**:80−3.
4. Jiao T, Yao X, Zhao Y, Zhou Y, Gao Y, Fan S, et al. Dexamethasone-induced liver enlargement is related to PXR/YAP activation and lipid accumulation but not hepatocyte proliferation. *Drug Metab Dispos* 2020;**48**:830−9.
5. Luo G, Cunningham M, Kim S, Burn T, Lin J, Sinz M, et al. CYP3A4 induction by drugs: correlation between a pregnane X receptor reporter gene assay and CYP3A4 expression in human hepatocytes. *Drug Metab Dispos* 2002;**30**:795−804.
6. Meng Z, Gwag T, Sui Y, Park SH, Zhou X, Zhou C. The atypical antipsychotic quetiapine induces hyperlipidemia by activating intestinal PXR signaling. *JCI Insight* 2019;**4**:e125657.
7. Rysä J, Buler M, Savolainen MJ, Ruskoaho H, Hakkola J, Hukkanen J. Pregnane X receptor agonists impair postprandial glucose tolerance. *Clin Pharmacol Ther* 2013;**93**:556−63.
8. Phabphal K, Limapichat K, Sathirapanya P, Setthawatcharawanich S, Geater A. Characterization of glucose homeostasis and lipid profile in adult, seizure-free, epileptic patients in Asian population. *Eur J Neurol* 2012;**19**:1228−34.
9. Vyas AK, Koster JC, Tzekov A, Hruz PW. Effects of the HIV protease inhibitor ritonavir on GLUT4 knock-out mice. *J Biol Chem* 2010;**285**:36395−400.
10. Kapse S, Ando H, Fujiwara Y, Suzuki C, Ushijima K, Kitamura H, et al. Effect of a dosing-time on quetiapine-induced acute hyperglycemia in mice. *J Pharmacol Sci* 2017;**133**:139−45.
11. Yamakawa T, Takano T, Tanaka S, Kadonosono K, Terauchi Y. Influence of pitavastatin on glucose tolerance in patients with type 2 diabetes mellitus. *J Atherosclerosis Thromb* 2008;**15**:269−75.
12. Takano T, Yamakawa T, Takahashi M, Kimura M, Okamura A. Influences of statins on glucose tolerance in patients with type 2 diabetes mellitus. *J Atherosclerosis Thromb* 2006;**13**:95−100.
13. Stage TB, Damkier P, Christensen MM, Nielsen LB, Højlund K, Brøsen K. Impaired glucose tolerance in healthy men treated with St. John's wort. *Basic Clin Pharmacol Toxicol* 2016;**118**:219−24.
14. Ling Z, Shu N, Xu P, Wang F, Zhong Z, Sun B, et al. Involvement of pregnane X receptor in the impaired glucose utilization induced by atorvastatin in hepatocytes. *Biochem Pharmacol* 2016;**100**:98−111.
15. Hassani-Nezhad-Gashti F, Rysä J, Kummu O, Näpänkangas J, Buler M, Karpale M, et al. Activation of nuclear receptor PXR impairs glucose tolerance and dysregulates GLUT2 expression and subcellular localization in liver. *Biochem Pharmacol* 2018;**148**:253−64.
16. Pavek P. Pregnane X receptor (PXR)-mediated gene repression and cross-talk of PXR with other nuclear receptors *via* coactivator interactions. *Front Pharmacol* 2016;**7**:456.
17. Gao J, Xie W. Targeting xenobiotic receptors PXR and CAR for metabolic diseases. *Trends Pharmacol Sci* 2012;**33**:552−8.
18. Sun B, Zhong Z, Wang F, Xu J, Xu F, Kong W, et al. Atorvastatin impaired glucose metabolism in C2C12 cells partly *via* inhibiting cholesterol-dependent glucose transporter 4 translocation. *Biochem Pharmacol* 2018;**150**:108−19.
19. Thorens B. GLUT2, glucose sensing and glucose homeostasis. *Diabetologia* 2015;**58**:221−32.
20. Chadt A, Al-Hasani H. Glucose transporters in adipose tissue, liver, and skeletal muscle in metabolic health and disease. *Pflügers Archiv* 2020;**472**:1273−98.
21. Cherrington AD. Banting Lecture 1997. Control of glucose uptake and release by the liver *in vivo*. *Diabetes* 1999;**48**:1198−214.
22. Moore MC, Coate KC, Winnick JJ, An Z, Cherrington AD. Regulation of hepatic glucose uptake and storage *in vivo*. *Adv Nutr* 2012;**3**:286−94.
23. Sala-Rabanal M, Hirayama BA, Ghezzi C, Liu J, Huang SC, Kepe V, et al. Revisiting the physiological roles of SGLTs and GLUTs using positron emission tomography in mice. *J Physiol* 2016;**594**:4425−38.
24. Burcelin R, Dolci W, Thorens B. Glucose sensing by the hepatoportal sensor is GLUT2-dependent: *in vivo* analysis in GLUT2-null mice. *Diabetes* 2000;**49**:1643−8.
25. Guillam MT, Burcelin R, Thorens B. Normal hepatic glucose production in the absence of GLUT2 reveals an alternative pathway for glucose release from hepatocytes. *Proc Natl Acad Sci U S A* 1998;**95**:12317−21.
26. Guillam MT, Hummler E, Schaerer E, Yeh JI, Birnbaum MJ, Beermann F, et al. Early diabetes and abnormal postnatal pancreatic islet development in mice lacking Glut-2. *Nat Genet* 1997;**17**:327−30.

27. Seyer P, Vallois D, Poitry-Yamate C, Schütz F, Metref S, Tarussio D, et al. Hepatic glucose sensing is required to preserve β cell glucose competence. *J Clin Invest* 2013;**123**:1662−76.
28. Kodama S, Yamazaki Y, Negishi M. Pregnane X receptor represses *HNF4α* gene to induce insulin-like growth factor-binding protein IGFBP1 that alters morphology of and migrates HepG2 cells. *Mol Pharmacol* 2015;**88**:746−57.
29. Hakkola J, Rysä J, Hukkanen J. Regulation of hepatic energy metabolism by the nuclear receptor PXR. *Biochim Biophys Acta* 2016;**1859**:1072−82.
30. Bhalla S, Ozalp C, Fang S, Xiang L, Kemper JK. Ligand-activated pregnane X receptor interferes with HNF-4 signaling by targeting a common coactivator PGC-1alpha. Functional implications in hepatic cholesterol and glucose metabolism. *J Biol Chem* 2004;**279**:45139−47.
31. Yeh MM, Bosch DE, Daoud SS. Role of hepatocyte nuclear factor 4-alpha in gastrointestinal and liver diseases. *World J Gastroenterol* 2019;**25**:4074−91.
32. Zhang W, Sargis RM, Volden PA, Carmean CM, Sun XJ, Brady MJ. PCB 126 and other dioxin-like PCBs specifically suppress hepatic PEPCK expression *via* the aryl hydrocarbon receptor. *PLoS One* 2012;**7**:e37103.
33. Ling Z, Xu P, Zhong Z, Wang F, Shu N, Zhang J, et al. Sensitive determination of glucose in Dulbecco's modified Eagle medium by high-performance liquid chromatography with 1-phenyl-3-methyl-5-pyrazolone derivatization: application to gluconeogenesis studies. *Biomed Chromatogr* 2016;**30**:601−5.
34. Shukla SK, Mulder SE, Singh PK. Hypoxia-mediated *in vivo* tumor glucose uptake measurement and analysis. *Methods Mol Biol* 2018;**1742**:107−13.
35. Celeng C, de Keizer B, Merkely B, de Jong P, Leiner T, Takx RAP. PET molecular targets and near-infrared fluorescence imaging of atherosclerosis. *Curr Cardiol Rep* 2018;**20**:11.
36. de Oliveira C, Patel K, Mishra V, Trivedi RN, Noel P, Singh A, et al. Characterization and predictive value of near infrared 2-deoxyglucose optical imaging in severe acute pancreatitis. *PLoS One* 2016;**11**:e0149073.
37. Pelletier L, Rebouissou S, Paris A, Rathahao-Paris E, Perdu E, Bioulac-Sage P, et al. Loss of hepatocyte nuclear factor 1alpha function in human hepatocellular adenomas leads to aberrant activation of signaling pathways involved in tumorigenesis. *Hepatology* 2010;**51**:557−66.
38. Hoffart E, Ghebreghiorghis L, Nussler AK, Thasler WE, Weiss TS, Schwab M, et al. Effects of atorvastatin metabolites on induction of drug-metabolizing enzymes and membrane transporters through human pregnane X receptor. *Br J Pharmacol* 2012;**165**:1595−608.
39. Wu H, Deng X, Shi Y, Su Y, Wei J, Duan H. PGC-1α, glucose metabolism and type 2 diabetes mellitus. *J Endocrinol* 2016;**229**:R99−115.
40. Yoon JC, Puigserver P, Chen G, Donovan J, Wu Z, Rhee J, et al. Control of hepatic gluconeogenesis through the transcriptional coactivator PGC-1. *Nature* 2001;**413**:131−8.
41. Li T, Chiang JY. Mechanism of rifampicin and pregnane X receptor inhibition of human cholesterol 7 alpha-hydroxylase gene transcription. *Am J Physiol Gastrointest Liver Physiol* 2005;**288**:G74−84.
42. Hukkanen J, Hakkola J, Rysa J. Pregnane X receptor (PXR)—a contributor to the diabetes epidemic?. *Drug Metabol Drug Interact* 2014;**29**:3−15.
43. Wang H, Maechler P, Antinozzi PA, Hagenfeldt KA, Wollheim CB. Hepatocyte nuclear factor 4α regulates the expression of pancreatic β-cell genes implicated in glucose metabolism and nutrient-induced insulin secretion. *J Biol Chem* 2000;**275**:35953−9.
44. Stoffel M, Duncan SA. The maturity-onset diabetes of the young (MODY1) transcription factor HNF4α regulates expression of genes required for glucose transport and metabolism. *Proc Natl Acad Sci U S A* 1997;**94**:13209−14.
45. Cha JY, Kim H, Kim KS, Hur MW, Ahn Y. Identification of transacting factors responsible for the tissue-specific expression of human glucose transporter type 2 isoform gene. Cooperative role of hepatocyte nuclear factors 1α and 3β. *J Biol Chem* 2000;**275**:18358−65.
46. Ban N, Yamada Y, Someya Y, Miyawaki K, Ihara Y, Hosokawa M, et al. Hepatocyte nuclear factor-1α recruits the transcriptional co-activator p300 on the *GLUT2* gene promoter. *Diabetes* 2002;**51**:1409−18.
47. Tan Y, Adami G, Costa RH. Maintaining HNF6 expression prevents AdHNF3β-mediated decrease in hepatic levels of Glut-2 and glycogen. *Hepatology* 2002;**35**:790−8.
48. Párrizas M, Maestro MA, Boj SF, Paniagua A, Casamitjana R, Gomis R, et al. Hepatic nuclear factor 1-alpha directs nucleosomal hyperacetylation to its tissue-specific transcriptional targets. *Mol Cell Biol* 2001;**21**:3234−43.
49. Agius L. Glucokinase and molecular aspects of liver glycogen metabolism. *Biochem J* 2008;**414**:1−18.
50. Song Y, Sui T, Zhang Y, Wang Y, Chen M, Deng J, et al. Genetic deletion of a short fragment of glucokinase in rabbit by CRISPR/Cas9 leading to hyperglycemia and other typical features seen in MODY-2. *Cell Mol Life Sci* 2020;**77**:3265−77.
51. Spruiell K, Richardson RM, Cullen JM, Awumey EM, Gonzalez FJ, Gyamfi MA. Role of pregnane X receptor in obesity and glucose homeostasis in male mice. *J Biol Chem* 2014;**289**:3244−61.
52. Kodama S, Moore R, Yamamoto Y, Negishi M. Human nuclear pregnane X receptor cross-talk with CREB to repress cAMP activation of the glucose-6-phosphatase gene. *Biochem J* 2007;**407**:373−81.
53. Gotoh S, Negishi M. Serum- and glucocorticoid-regulated kinase 2 determines drug-activated pregnane X receptor to induce gluconeogenesis in human liver cells. *J Pharmacol Exp Therapeut* 2014;**348**:131−40.
54. Gotoh S, Negishi M. Statin-activated nuclear receptor PXR promotes SGK2 dephosphorylation by scaffolding PP2C to induce hepatic gluconeogenesis. *Sci Rep* 2015;**5**:14076.
55. Jiang Y, Feng D, Ma X, Fan S, Gao Y, Fu K, et al. Pregnane X receptor regulates liver size and liver cell fate by Yes-associated protein activation in mice. *Hepatology* 2019;**69**:343−58.
56. Yao XP, Jiao TY, Jiang YM, Fan SC, Zhao YY, Yang X, et al. PXR mediates mifepristone-induced hepatomegaly in mice. *Acta Pharmacol Sin* 2022;**43**:146−56.
57. Huck I, Gunewardena S, Espanol-Suner R, Willenbring H, Apte U. Hepatocyte nuclear factor 4 alpha activation is essential for termination of liver regeneration in mice. *Hepatology* 2019;**70**:666−81.
58. Walesky C, Gunewardena S, Terwilliger EF, Edwards G, Borude P, Apte U. Hepatocyte-specific deletion of hepatocyte nuclear factor-4α in adult mice results in increased hepatocyte proliferation. *Am J Physiol Gastrointest Liver Physiol* 2013;**304**:G26−37.
59. Wu H, Reizel T, Wang YJ, Lapiro JL, Kren BT, Schug J, et al. A negative reciprocal regulatory axis between cyclin D1 and HNF4α modulates cell cycle progression and metabolism in the liver. *Proc Natl Acad Sci U S A* 2020;**117**:17177−86.
60. Gupta RK, Vatamaniuk MZ, Lee CS, Flaschen RC, Fulmer JT, Matschinsky FM, et al. The MODY1 gene HNF-4α regulates selected genes involved in insulin secretion. *J Clin Invest* 2005;**115**:1006−15.
61. Miura A, Yamagata K, Kakei M, Hatakeyama H, Takahashi N, Fukui K, et al. Hepatocyte nuclear factor-4α is essential for glucose-stimulated insulin secretion by pancreatic β-cells. *J Biol Chem* 2006;**281**:5246−57.